Performance Optimized Approach for Automatic Fiducial Segmentation in Medical Imaging to Assist Robot-guided Neurosurgery

Shwetank Panwar
Dept. of Bioscience and Bioengineering
Indian Institute of Technology
Guwahati, India
panwar1997shwetank@iitg.ac.in

Cota Navin Gupta
Dept. of Bioscience and Bioengineering
Indian Institute of Technology
Guwahati, India
cngupta@iitg.ac.in

***Abstract*—Registration of patient head with the surgical planning software is crucial for attaining precision in autonomous robot-guided neurosurgery. The most minimally invasive registration approach is to use skin-attached fiducial markers and segmenting these markers in MRI/CT modality images to accurately register them in a physical-coordinate system. While the past approaches to segment and localize these markers have improved in accuracy, they have become increasingly complex and computationally heavy over time. Our proposed approach tackles this problem and maintain a balance in terms of both accuracy and speed. We propose three major improvements for cutting down the iterations required in the computation - 1. Down-sampling the image space through max-pooling optimization, 2. Applying convolutional filter search in this space and 3. Mapping the searched seed points back to original image for performing clustering. Our algorithm attained reasonable localization accuracy on phantom-skull CT as well as simulated sMRI scan and needed very less computational time compared to past approaches. All fiducial markers- 14 in phantom CT and 6 in simulated sMRI were successfully clustered and localized.**

***Index Terms*—Robot-guided Neurosurgery, Fiducial Localization, Max-Pooling, Convolution filter**

I. Introduction

Development of modern instrumentation and computation techniques have led to some incredible advancements in the field of robot-guided neurosurgical systems. These surgical systems utilizes prior knowledge of patients head anatomy with an image-guided system. Registration of patient with the surgery-planning software is crucial to attain surgical precision. Images of the patient obtained through modalities like MRI and CT are utilized for registration purpose. In this procedure, CT or MRI scan of patient is performed with physical markers called fiducials, attached to patients head. These markers are segmented in the 3D medical image and their center coordinate is used to perform registration with the surgical system.

So far, these fiducial markers are the most minimally invasive method of patient registration. Even today, most advanced surgical robots such as STAR relies on manual registration of patient by a human operator [1]. This makes the registration process susceptible to human error. While approaches proposed in the past to automatically register fiducials marker are quite accurate, they are computationally intensive. This increases the resources required by these algorithms and ultimately their hardware cost. These past approaches can be understood in 3 broad categories 1) Searching for fiducial projections in 2D slices of the 3D volume, 2) Applying morphological operations and hand-crafted filters for cross-correlation in 2D as well as 3D image space and 3) Surfaces extraction from 3D volume and performing an extensive search for marker geometry.

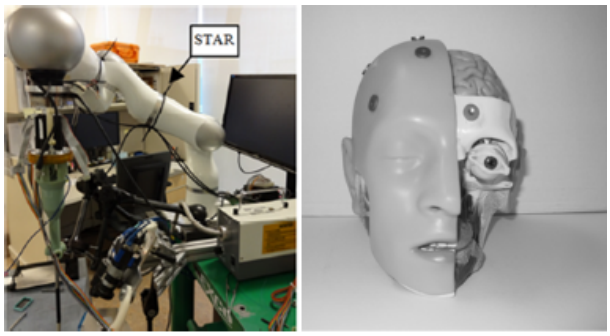

Fig. 1. STAR surgical robot(left) [1], Fiducial markers attached to the phantom skull(right) [3]

The first approach proposed by Chen et. al. uses curve fitting and template matching across all the 2D slices of the 3D volume [2]. The major problem with this approach is that certain markers might not have their proper detectable projections in 2D space [2]. This sometimes gives false positive results. The second approach proposed by Terry et. al. is computationally heavy and time consuming because of its use of morphological operations in 3D space [3]. Another approach in the second category uses hand-crafted correlation filters to obtain regions with maximum confidence for markers but this approach is also inaccurate and produce false positive results [4]. The third approach proposed by Fattori et. al. employs graphical processing, as well as, isosurface extraction

[5], making it unfit to run on low-end systems. Therefore, we need an algorithm that provides decent registration accuracy, as well as, computation speed while performing the localization operation.

Our proposed approach achieves this balance by searching the fiducial markers in downsampled image space for fiducial seeds and then mapping these seeds back to the original image. There is no need to search for seed points for segmentation in the entire image space when the points can be easily mapped back to the original space by a linear transformation.

The algorithm we propose works in the following sequence: 1) Searching for circular points in the initial 2D slices of the volume and determining the intensity range for fiducials. 2) Down-sampling the image space through pooling operation. 3) Clipping the image region out of intensity range and applying Otsu thresholding method. 4) Applying convolution filter to find dense regions with fiducial voxels. 5) Mapping the searched points back to original image space and performing clustering. Each step will be explained in the later sections.

II. Methodology

A. Circle Detection in Initial Slices

This first step in the process plays a crucial role in obtaining knowledge about fiducial intensity range and its voxel volume. These parameters are essential for cross-validation to avoid false-positive results. As we can observe in the Fig. 2, the cylindrical markers appear as circles in the initial slices. We apply Hough circle transformation [6] to the first 20 slices for finding fiducials. Houghs method parametrizes the pixels with the following equation:

$$(x-a)^2 + (y-b)^2 = R^2 \tag{1}$$

where a,b are coordinates and R is radius of circle.

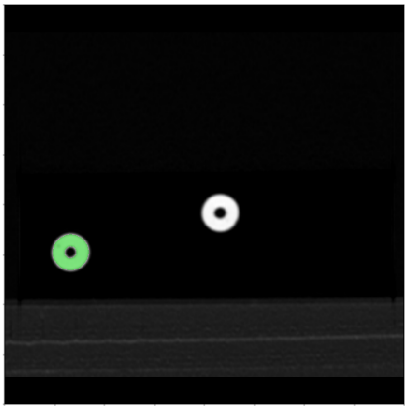

Fig. 2. Fiducial markers visible as circles in initial slices of the image volume.

B. Image Downsampling

A typical MRI or CT scan may vary in volume from 100 to 250 voxels in one of the three dimensions. Such volume size makes any 3D spatial search algorithm to become highly expensive in terms of computation. As shown in Fig. 3, pooling can downsize our feature space while maintaining the vital features. We have used max-pooling with zero padding and stride of 3 for this purpose:

$$A'_{ij} = max\left\{a_{kl} \in A\right\} \tag{2}$$

where A' is the downsampled image and A is the region inside pooling window.

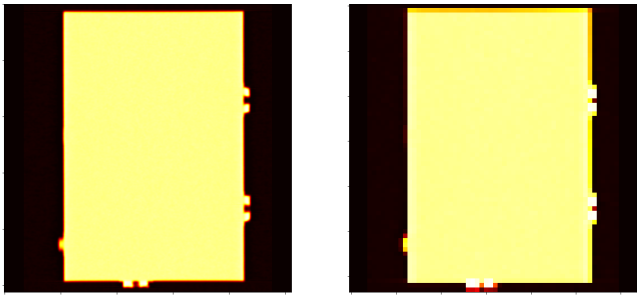

Fig. 3. Original image(left), Image downsampled by Max-Pooling(right)

C. Global Thresholding Operations

Before thresholding, we clip the voxels outside the intensity range of fiducial markers as shown in Fig. 4. Even after clipping, some noisy voxels are still present. These voxels can be minimized using the method proposed by Nobuyuki Otsu, also known as 'Otsu thresholding' [7]. In this approach, we try to minimize intra-class variance, defined as a weighted sum of variances of the two clustered classes:

$$\sigma_w^2(t) = \omega_0(t)\sigma_0^2 + \omega_1(t)\sigma_1^2 \tag{3}$$

Weights ω_0 and ω_1 are the probability of the two classes separated by a threshold t and σ_0,σ_1 are variances of these two classes.

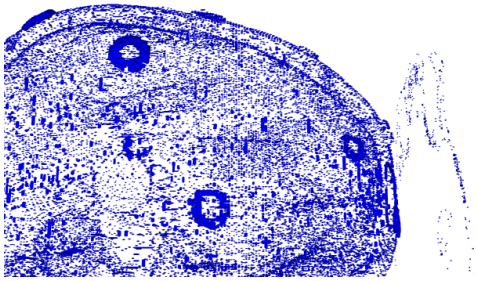

Fig. 4. Noisy voxels visible in the image apart from the dense fiducial markers after thresholding. Source: BARC Phantom CT skull dataset.

D. Convolutional search

Once we obtain a binary image after thresholding, it is necessary to obtain the seeding voxels for segmentation of the whole fiducial in the original image space. To search for

dense fiducial regions, we apply a simple convolution filter on this image [8].

$$I' = I \otimes F \tag{4}$$

The convolution operation (4) can be simply understood in the following form:

$$I' = \sum_{a=0}^{i-1} \sum_{b=0}^{j-1} \sum_{c=0}^{k-1} I[m-a, n-b, o-c] \cdot F[a, b, c] \tag{5}$$

Here, I'is the output matrix obtained after the convolution of image matrix I and spherical structuring element kernel F of dimensions [5,5,5](used in this case). While choosing the kernel size, we kept it slightly bigger than a fiducial marker dimensions in downsampled image to capture the dense point cloud around fiducials. Next, we find the points of local maxima inside the matrix obtained after convolution [9].

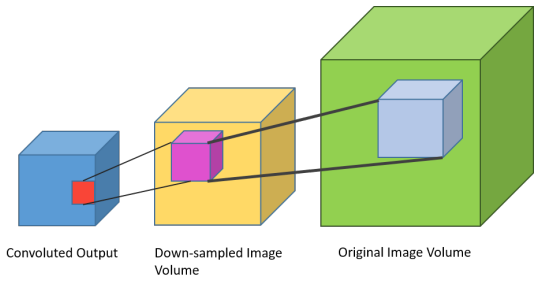

Fig. 5. Mapping the coordinate back to the original image.

The process of mapping the coordinates back to original image is shown in Fig. 5. We start the mapping process from the convolution output array with the points of local maxima inside it(as visible in Fig. 6). The region corresponding to these point is mapped back to the downsampled image from where the mapped region is again inverse-mapped back to the original image space. Again, a voxel point lying in the intensity range of the fiducial marker is taken and clustering starts as per the process explained in the section E.

E. Clustering

In order to cluster the fiducial markers, we consider the fiducial seed voxel as the center of the sphere with diameter D obtained from the circle detection step. We achieve the clustering of the whole fiducial in these steps:

1) Initialize the radius of the sphere as R = 0.
2) Keep increasing the radius and select the points with same intensity range as the fiducial marker.
3) Repeat the process until R = D.
4) Check whether the volume of cluster V' is equal to fiducial volume V.
5) If V' == V, then count as a fiducial point. Else, reject the cluster.
6) Repeat the steps 1-5 for another seed point.

Similar clustering approach is available in ITK toolkit library as Connected Threshold Image Filter which can be utilized in case of more complex cluster shapes [10].

F. Localization

In order to find the fiducial center of the markers for registration process, we calculate the intensity weighted centroid coordinates(X,Y,Z) by taking into consideration the intensity A(x,y,z) of the corresponding voxel coordinates.

$$X = \frac{\sum_{i=0}^{i_{max}} x_i A(x_i)}{\sum_{i=0}^{i_{max}} A(x_i)} ; A(x_i) = \sum_{j=0}^{j_{max}} \sum_{k=0}^{k_{max}} I(x_i, y_j, z_k) \tag{6}$$

$$Y = \frac{\sum_{j=0}^{j_{max}} y_j A(y_j)}{\sum_{j=0}^{j_{max}} A(y_j)} ; A(y_j) = \sum_{i=0}^{i_{max}} \sum_{k=0}^{k_{max}} I(x_i, y_j, z_k) \tag{7}$$

$$Z = \frac{\sum_{k=0}^{k_{max}} z_k A(z_k)}{\sum_{k=0}^{k_{max}} A(z_k)} ; A(z_i) = \sum_{j=0}^{j_{max}} \sum_{k=0}^{k_{max}} I(x_i, y_j, z_k) \tag{8}$$

where (x_i, y_i, z_i) and $I(x_i, y_i, z_i)$ are coordinates and corresponding intensity values in the fiducial cluster, and i_{max}, j_{max} and k_{max} are the no. of voxels in the X,Y and Z direction of the fiducial cluster respectively.

III. Results and Observations

We tested our approach on two Bhabha Atomic Research Center(BARC) datasets of different modalities and no. of fiducial markers as given in Table I. Shape of fiducial marker was cylindrical in both the datasets. The first dataset consisted of CT scan of phantom skull with fiducial markers attached to it. The second dataset was prepared through simulation and consists of a cuboidal box with cylindrical fiducials attached to it. Both of these datasets are part of Project RATHNA, Bhabha Atomic Research Center(BARC) [11].

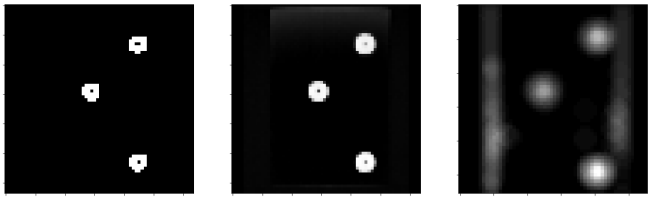

Fig. 6. Original image(left), Max-pooled image(center), Output array after convolution(right). Source: BARC Simulated MRI dataset

IV. Conclusion

As shown in Fig. 7 and Fig. 8, all the fiducial markers in both the datasets were successfully clustered and localized using our proposed approach. The algorithm provided decent detection accuracy while being less computationally expensive

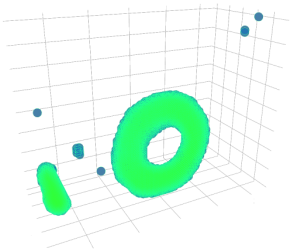

Fig. 7. Clustered fiducial marker in BARC phantom skull dataset.

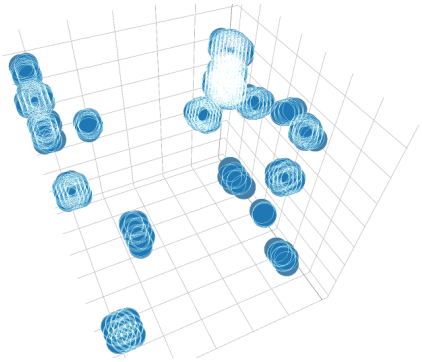

Fig. 8. Clustered regions in the BARC phantom skull dataset.

TABLE I
TEST DATASETS AND THEIR INFORMATION.

Name	No. of Fiducials	Dimensions	Diameter(mm)
Phantom skull	14	512*512*144	12.5
Simulated dataset	6	512*512*720	12.5

TABLE II
ALGORITHM RUNTIME

Algorithm	CPU	Time(seconds)
Proposed Approach	Intel i3-5th Gen	90.5
Surface processing[5]	Intel i7-820QM Gen	50

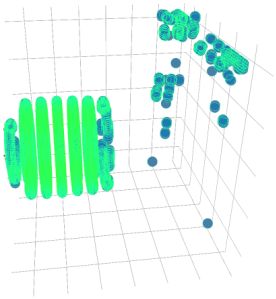

Fig. 9. Clustered fiducial marker in the BARC simulated MRI dataset with some error points clustered at the right.

and time consuming. Even on the simulated dataset, it took around 90.6 s for complete run on Intel i3 CPU. According to [5], the surface processing approach took nearly 50.0 s to run on i7 system, which is nearly close to our algorithm.(See Table II)

As shown in Fig. 9, the algorithm clustered some erroneous voxels in some clusters which might be due to the similar intensity levels of these error voxels. This lead to some deviation from the actual fiducial centroid coordinate. Robustness of the algorithm can be increased by using connectivity threshold filter which works on neighbourhood connectivity detection.

FUTURE SCOPE OF WORK

Our algorithm tackles the specific problem of localizing fiducial markers in a 3D volume. This problem can be further generalized as the segmentation problem in multi-dimensional space and can be approached using ICA and Neural Networks.

ACKNOWLEDGMENT

We would like to express our sincere gratitude towards Bhabha Atomic Research Center(BARC), India for providing us with their high-quality datasets. We are also grateful to the Dept. of Bioscience and Bioengineering at IIT Guwahati for providing access to their BIF Servers and funding this work.

REFERENCES

[1] J. D. Opfermann et al., "Semi-autonomous electrosurgery for tumor resection using a multi-degree of freedom electrosurgical tool and visual servoing," 2017 IEEE/RSJ International Conference on Intelligent Robots and Systems (IROS), Vancouver, BC, 2017, pp. 3653-3660.

[2] Chen, Dingguo, et al. "Automatic fiducial localization in brain images." International Journal of Computer Assisted Radiology and Surgery 1 (2006): 45.

[3] Gu, Lixu, and Terry Peters. "3D automatic fiducial marker localization approach for frameless stereotactic neuro-surgery navigation." International Workshop on Medical Imaging and Virtual Reality. Springer, Berlin, Heidelberg, 2004.

[4] D. Walvoord, K. G. Baum, M. Helguera, A. Krol and R. Easton, "Localization of fiducial skin markers in MR images using correlation pattern recognition for PET/MRI nonrigid breast image registration," 2008 37th IEEE Applied Imagery Pattern Recognition Workshop, Washington DC, 2008, pp. 1-4.

[5] G. Fattori et al., "Automated Fiducial Localization in CT Images Based on Surface Processing and Geometrical Prior Knowledge for Radiotherapy Applications," in IEEE Transactions on Biomedical Engineering, vol. 59, no. 8, pp. 2191-2199, Aug. 2012.

[6] H. Ye, G. Shang, L. Wang and M. Zheng, "A new method based on hough transform for quick line and circle detection," 2015 8th International Conference on Biomedical Engineering and Informatics (BMEI), Shenyang, 2015, pp. 52-56.

[7] Yuncong Feng, Haiying Zhao, Xiongfei Li, Xiaoli Zhang, Hongpeng Li, A multi-scale 3D Otsu thresholding algorithm for medical image segmentation, Digital Signal Processing, Volume 60, 2017, Pages 186-199, ISSN 1051-2004.

[8] Rafael C. Gonzalez, Richard Eugene Woods, Digital Image Processing, 3rd Edition, 1996.

[9] Wei-Mei Chen, Hsien-Kuei Hwang, Tsung-Hsi Tsai, Maxima-finding algorithms for multidimensional samples: A two-phase approach, Computational Geometry, Volume 45, Issues 12, 2012, Pages 33-53.

[10] Jiang, Huiyan, et al. "A region growing vessel segmentation algorithm based on spectrum information." Computational and mathematical methods in medicine 2013 (2013).

[11] Bhutani, Gaurav, et al. "Neuro-Registration and Navigation Unit for Surgical Manipulation." Proceedings of the 1st International and 16th National Conference on Machines and Mechanisms, IIT Roorkee, India. 2013.